Quasi-Elastic Light Scattering from Ternary Mixtures of Poly(methyl methacrylate)/Poly(dimethylsiloxane) in Tetrahydrofuran

L. Giebel, R. Borsali,*,† E. W. Fischer, and G. Meier

Max-Planck-Institut für Polymerforschung, Postfach 3148, D-6500, Mainz, Federal Republic of Germany

Received December 21, 1989; Revised Manuscript Received March 13, 1990

ABSTRACT: The dynamic behavior of the ternary mixture poly(methyl methacrylate)/poly(dimethylsiloxane)/tetrahydrofuran (PMMA/PDMS/THF), where THF and PDMS are isorefractive, has been investigated by quasi-elastic light scattering (QELS). Two distinct modes have been observed in the autocorrelation function of the scattered light. In the semidilute range at one total polymer concentration $C_T > C^*$ (where C^* is the overlap concentration) and far from the "cloud point" $C_T < C_{sp}$ (where C_{sp} is the spinodal concentration), the variation of the two relaxation processes characterized by their frequencies Γ_C and Γ_I and their amplitudes a_C and a_I has been examined as a function of the relative composition of the "visible" polymer (e.g., PMMA) $x = C_{PMMA}/C_T$ and the scattering vector q. The experimental results are in good agreement with recent theoretical calculations based on the random phase approximation (RPA) developed by Benoit and Benmouna. Indeed, the first mode, Γ_C, which is fast, is independent of the composition and characterizes the total concentration fluctuations. Its value is identical with that measured in the corresponding binary system (e.g., PMMA/THF); it is the cooperative diffusion coefficient mode. The second mode, Γ_I, which is slow, is sensitive to the composition. It describes the motion of one species with respect to the other and is called the interdiffusion mode. As regards the amplitudes a_C and a_I of these two processes, the experimental results show a sensitive variation with the relative composition x according to the theoretical predictions.

Introduction

Over the past decade, there has been considerable interest in the dynamic properties of polymer mixtures in bulk[1-11] and in solution[12-17] from both theoretical and experimental points of view. Experimental methods used include forced Rayleigh scattering (FRS), pulsed-field-gradient NMR (PFG-NMR), and quasi-elastic light scattering (QELS). With QELS in solution, the solvent is always chosen to be isorefractive with one of the polymers. The idea is that the dynamics are then driven by the "visible" polymer and the interpretation is easier. At small concentrations of the probe, one observes its self-diffusion coefficient at a finite concentration of the "invisible" polymer, which is the matrix. Several types of mixtures have been considered. Polystyrene/poly(vinyl methyl ether) (PS/PVME)[18-28] in toluene or in *o*-fluorotoluene (*o*-FT) was the most frequently studied system because of the high degree of compatibility between these two polymers. With such compatible systems, a wide range of molecular weights and concentrations has been explored, and some scaling laws for the self-diffusion coefficient have been deduced. Other polymer mixtures such as PS/PMMA/solvent[29-38] were considered in the framework of similar studies, but only a limited range of molecular weights and concentrations has been explored because of the incompatibility of these polymers. The ternary mixture PS_1/PS_2/solvent,[39-41] where the two polystyrenes differ only in their molecular weights, was also investigated over reasonable ranges of molecular weights and concentrations because of the compatibility of this system. All of the reported experiments dealt with a system far from the "cloud point" or the phase separation (spinodal decomposition). The common point of these studies was the use of a small composition of the "visible" polymer x in a matrix. Most of the experimental results on these systems showed a monoexponential behavior of the scattered autocorrelation function as measured by QELS except for a few cases where two modes were observed.[35,38,39] The aim of these studies was to verify if the only observed mode, which is slow, could be interpreted in terms of a reptation motion[42] or if other sophisticated dynamic processes[43] had to be taken into account. In spite of the great experimental effort expended, most of the reported results are still the subject of controversy.

More recently, using the random phase approximation (RPA) technique, Benoit, Benmouna, and co-workers[44-47] have published a series of papers in which they have developed a theory that is able to describe the dynamic behavior of two monodisperse polymers in a solvent. This may be the case of mixtures of two homopolymers in a solvent or diblock copolymer in solution. The details of the calculations and the applications of the theory have been presented in ref 48. In their calculations, they have shown that the autocorrelation function of the scattered intensity is the sum of two exponential functions characterized by relaxation frequencies Γ_C and Γ_I. These two processes have different physical meanings. Indeed, the first one, Γ_C, which is fast, depends on the excluded volume V, characterizes the total polymer concentration fluctuations, and has the same value as that measured in the corresponding binary system (i.e., polymer 1/solvent or polymer 2/solvent) at the identical total polymer concentration. It has been called the cooperative diffusion mode. The second one, Γ_I, which is slow, characterizes the composition fluctuations, depends on the Flory interaction parameter χ, and describes the motion of one species with respect to the other. It has been called the interdiffusion mode and is the only mode that survives in the bulk state.[1-11]

In this treatment, general expressions have been derived for the amplitudes and the frequencies of the two processes under various conditions of the thermodynamic parameters (i.e., excluded volume V and Flory-Huggins parameter χ), the molecular weight M_w, the total polymer concentration

* To whom correspondence should be addressed.
† CNRS-CERMAV, 53x, F-38041 Grenoble Cédex, France.

0024-9297/90/2223-4054$02.50/0

C_T, the composition of the "visible" polymer x, and the wave vector q. The relations that have been obtained are very useful for estimating the optimal experimental conditions necessary to observe these two processes simultaneously. As has been shown,[44] these ideal conditions correspond to (i) a total polymer concentration C_T such that $C < C_T < C_{sp}$ (i.e., the system is in a one-phase regime ($C_T < C_{sp}$) and in semidilute solution ($C_T > C^*$), where C_{sp} and C^* are the spinodal and the overlap concentrations, respectively) in order to obtain a value of the ratio Γ_C/Γ_I as large as possible (under this condition the two processes should be easily separated) and (ii) a relatively high value of the composition of the "visible" polymer x in order to have the amplitudes of these two processes in the same order of magnitude.

More recently and to check the validity of this theoretical treatment, two ternary systems were considered by Borsali et al.: PS/PMMA/toluene[49,50] and PS/PDMS/solvent[51] (THF, toluene). In these experimental studies, unlike those of other authors, the composition of the "visible" polymer, as discussed above, was chosen to be high; namely, $x = C_{PS}/C_T = 0.92$ in the case of PS/PMMA/toluene and $x = C_{PS}/C_T = 0.54$ in the case of PS/PDMS/THF. Two modes were indeed found. The values of the cooperative diffusion coefficients measured in the semidilute region for PS/PMMA/toluene and PS/PDMS/THF were equal to those obtained at identical polymer concentrations with the corresponding binary systems PS/toluene and PS/THF, respectively. The angular dependence of Γ_C and Γ_I was also investigated by the same authors,[48-51] and the results showed a q^2 dependence for Γ_C whereas Γ_I presents a significant deviation from q^2 behavior according to the theoretical variations. For both systems and at each composition, the cooperative diffusion coefficient $D_C = (\Gamma_C/q^2)_{q\to 0}$ increases with the total polymer concentration while the interdiffusion coefficient $D_I = (\Gamma_I/q^2)_{q\to 0}$ decreases when the total polymer concentration increases. As far as the amplitudes of these two modes are concerned, the experimental results show good agreement with the theoretical predictions. Without going into details, most of the experimental data obtained from the ternary mixtures PS/PMMA/toluene[49,50,52] and PS/PDMS/solvent[51] and, more recently, from the homopolymeric polyisobutylene system PIB_1/PIB_2/chloroform[53,54] (where PIB_1 and PIB_2 differ only in their molecular weights) were consistent with the mean-field theory based on the RPA developed by Benoit and Benmouna.[44]

As mentioned above, the choice of the composition of the "visible" polymer at a given total polymer concentration is important. It is one of the crucial points in this theory. Indeed, in the small range of composition $x < 0.1$ only one mode, which is slow, has been detected,[18-34,36,37,39,41] and at relatively high composition two modes characterize the dynamics.[35,38,48,54]

Our goal in this paper is to explore, at one total polymer concentration C_T (in the semidilute regime ($C_T > C^*$)) and far from the "cloud point" (e.g., in the one-phase regime ($C_T < C_{sp}$)), the whole range of composition ($0 < x \leq 1$) in order to see how the second process emerges when the composition increases. To do this, we have chosen the ternary mixture PMMA/PDMS/THF, where THF is isorefractive with PDMS. To our knowledge, this is the first time that such a system has been investigated by QELS. We note, however, that static measurements,[55] using classical light scattering, have already been done and were useful for our dynamic experiments. Before presenting our experimental results, we recall some of theoretical predictions describing the dynamic behavior of the ternary mixture P1/P2/solvent, especially in the case when the increment of refractice index of polymer 2, $(dn/d\phi)_2$, is equal to zero. In this case the total intermediate scattering function $S_T(q,t)$ reduced to

$$S_T(q,t) = S_{11}(q,t) = a_C e^{-\Gamma_C t} + a_I e^{-\Gamma_I t} \quad (1)$$

where $q = (4\pi/\lambda)n \sin(\theta/2)$, λ is the wavelength of the incident radiation, θ is the scattering angle, n is the refractive index of the medium, and t is the time. In this simple case, the theoretical expressions for the amplitudes a_C and a_I and the frequencies Γ_C and Γ_I of the two processes that characterize the dynamic behavior of the ternary mixture are[44,48,50,51]

$$a_C = x^2\Phi NP(q)\frac{1 - \chi/\chi_c(q)}{1 + V\Phi NP(q)[1 - \chi/\chi_c(q)]} \quad (2)$$

$$a_I = x(1-x)\Phi NP(q)\frac{1 + V\Phi NP(q)}{1 + V\Phi NP(q)[1 - \chi/\chi_c(q)]} \quad (3)$$

$$\Gamma_C = \Gamma_S(q)[1 + V\Phi NP(q)] \quad (4)$$

$$\Gamma_I = \Gamma_S(q)[1 - \chi/\chi_c(q)] \quad (5)$$

where

$$\chi_c(q) = [2x(1-x)\Phi NP(q)]^{-1} \quad (6)$$

In these relations, it is assumed that the solvent has the same quality for both polymers (e.g., the same excluded volume: $V_{11} = V_{22} = V$) and a small interaction χ between the two species, which is taken into account by the quantity $V_{12} = V + \chi$, where $\chi \ll V$. For the sake of simplicity it is assumed also that the two polymers have the same dimension, $R_{g,1} = R_{g,2} = R_g$ [i.e., the same form factor $P_1(q) = P_2(q) = P(q)$], and the same degree of polymerization, $N_1 = N_2 = N$. Φ, x, and $\chi_c(q)$ are the total polymer concentration, the composition of the "visible" polymer, and the critical interaction parameter, respectively. In relations 4 and 5, $\Gamma_S(q)$ is the self-relaxation frequency. In the semidilute regime $C_T > C^*$, the hydrodynamic interactions are screened and the expression for $\Gamma_S(q)$ in the Rouse model[56] is

$$\Gamma_S(q) = q^2\left(\frac{kT}{N\zeta}\right)\frac{1}{P(q)} = q^2\frac{D_S}{P(q)} \quad (7)$$

where k is the Boltzmann constant, T is the absolute temperature, $D_S = (kT/N\zeta)$ is the self-diffusion coefficient, and ζ is the friction coefficient of a monomer unit. ζ is assumed to be the same for both monomer units, and therefore D_S reflects the self-diffusion coefficient of each polymer. Figure 1 recalls the theoretical variation of the relative amplitude of the fast mode, $a_C/(a_C + a_I)$, as a function of the composition x of the "visible" polymer at the total polymer concentrations C^* (curve a) and $10C^*$ (curve b) at $\chi/V = 0.1$ and $P(q) = 1$. From an experimental point of view it is useful to recall that in the standard notation $V\Phi N = 2A_2M_wC_T$ and C^* corresponds approximately to $A_2M_wC^* = 1$ (A_2, M_w, and C_T are the second virial coefficient, the molecular weight, and the total polymer concentration, respectively). As regards the frequencies we have plotted in Figure 2, in arbitrary units, the theoretical variations of the two diffusion coefficients $D_C = (\Gamma_C/q^2)_{q\to 0}$ and $D_I = (\Gamma_I/q^2)_{q\to 0}$ as a function of the composition of the "visible" polymer x at the total polymer concentration $C_T = 10C^*$, which corresponds approximately to our experimental total polymer concentration. From this figure and according to relations 4–7, it may be seen that D_C is independent of x whereas D_I exhibits a sensitive

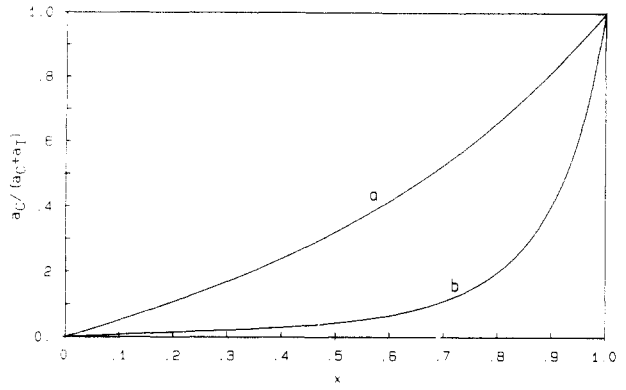

Figure 1. Theoretical variation of the relative amplitude of the fast mode $a_C/(a_C + a_I)$ as a function of the composition x of the "visible" polymer in ternary mixtures at $q = 0$ and $\chi/V = 0.1$: (a) $C_T = C^*$; (b) $C_T = 10C^*$.

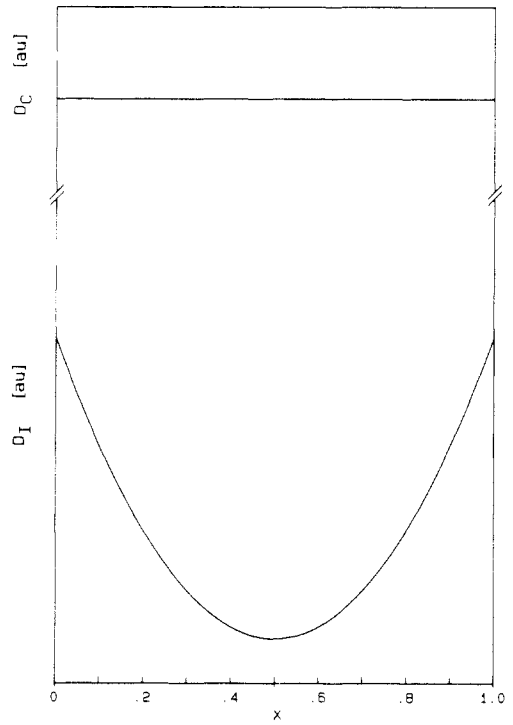

Figure 2. Theoretical variation of the cooperative diffusion coefficient D_C (a (top)) and the interdiffusion coefficient D_I (b (bottom)) as a function of composition x of the "visible" polymer in ternary mixtures at $q = 0$, $\chi/V = 0.1$, and $C_T = 10C^*$.

variation with the composition of the "visible" polymer. On the other hand, $D_I = (\Gamma_I/q^2)_{q\to 0}$ depends also on the total polymer concentration. It decreases when the total polymer concentration increases. Since D_I depends on x and C_T, it is interesting to illustrate this behavior in a three-dimensional plot. This is done in Figure 3, where the theoretical variation of $(D_I/D_S)_{q\to 0}$ is plotted as a function of composition x and total polymer concentration C_T at $\chi/V = 0.1$. This value of χ/V corresponds to our experimental results as we will show later. The quantities $V\Phi N$ and $\chi\Phi N$ have been replaced by $2A_2M_wC_T$ and $(\chi/V)(2A_2M_wC_T)$, respectively. If the concentration is too high, D_I becomes negative for some values of x and C_T (dashed lines). This means that the system cannot exist for these values of x and C_T as a homogeneous phase and corresponds to phase separation (via spinodal decomposition). In our system such a situation occurs for $x = 0.5$ at $C_T = (C_{sp})_{exp} \simeq 2.77 \times 10^{-2}$ g/cm^3 (see Figure 3).

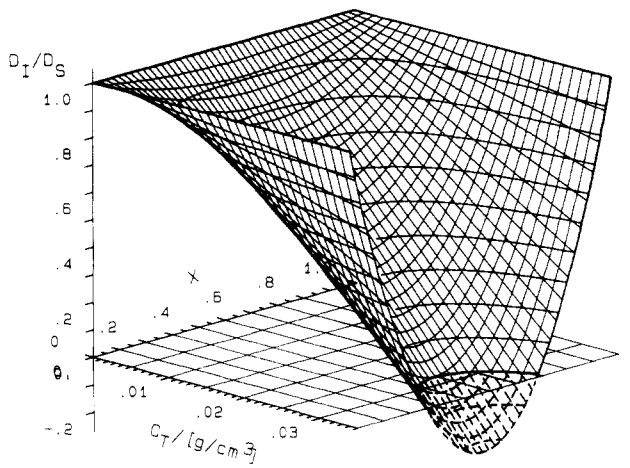

Figure 3. Theoretical variation in three-dimensional plot of the interdiffusion mode as a function of the composition x and the total polymer concentration C_T at $q = 0$ and $\chi/V = 0.1$.

Table I
Properties of Polymer Samples

sample	$M \times 10^{-3}$	$I = M_w/M_n$	R_g, Å	$A_2 \times 10^{-4}$, mol cm^3 g^{-2}
PMMA	730	1.13	583[a]	2.70[a]
PDMS	717	1.40	427[b]	2.75[c]

[a] From static light scattering measurements (PMMA/THF). [b] $R_g = (0.15 \pm 0.01)M_w^{0.59\pm0.01}$.[57] [c] $A_2 = (80 \pm 3) \times 10^{-4}M_w^{-0.25\pm0.01}$.[57]

Experimental Section

Materials and Sample Preparation. PMMA was obtained from Polymer Standards Service, Mainz, FRG, and PDMS was prepared in our laboratory. The characteristics of these polymers are given in Table I. The weight-average molecular weight M_w, the radius of gyration R_g, and the second virial coefficient A_2 of PMMA were determined by static light scattering measurements in THF. Those values for PDMS were calculated from the literature.[57] Several PMMA/PDMS/THF solutions were prepared at the same total polymer concentration $C_T = 1.33 \times 10^{-2}$ g/cm^3 in the range of composition of the "visible" polymer $x = C_{PMMA}/C_T$ ($0.1 < x \leq 1$). One notes that the overlap concentration[58] is approximately $C^* \simeq 0.14 \times 10^{-2}$ g/cm^3 and the concentration at the "cloud point" is approximately $C_{cp} \simeq 1.6 \times 10^{-2}$ g/cm^3 at $x = 0.5$. From the theoretical point of view this means that the properties of the system studied could be interpreted in the framework of the RPA. The solutions were allowed to mix during 3 weeks. They were filtered with 0.45-μm Millipore filters. Solutions were allowed to equilibrate for a few days following filtration and prior to measurements. The homogeneity of the solutions was tested by classical light scattering.

Equipment and Data Analysis. The full homodyne correlation function of the scattered intensity defined on 1023 channels was obtained by using the ALV-3000 autocorrelator from ALV, Langen, FRG. With such an autocorrelator it is possible to resolve, in one run, the underlying dynamics with high accuracy because of the 1023 available channels. The scattered light of a vertically polarized 4880-Å Ar ion laser (Spectra-Physics 2020) was measured at several angles in the range 50–130° at the temperature $t = 30.0 \pm 0.1$ °C. The total intermediate scattering function $S_T(q,t)$, which is reduced in this case to $S_{11}(q,t)$, is related to the measured homodyne intensity autocorrelation function $G^{(2)}(q,t)$ by the Siegert relation[59]

$$G^{(2)}(q,t) = B(1 + \alpha|S_{11}(q,t)|^2) \quad (8)$$

where B is the base line and α is the spatial coherence factor depending upon the geometry of the detection. The constrained regularization method (CONTIN) developed by Provencher[60] was used to obtain the distribution $A(\tau)$ of decay times. A statistical parameter "probability to reject" (P) is calculated for each solution,

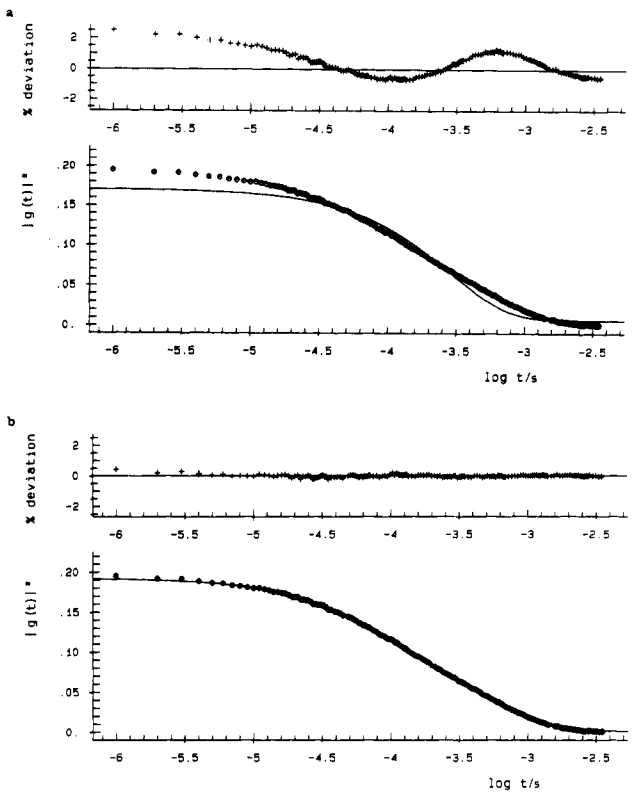

Figure 4. (a) Typical autocorrelation function as measured by QELS on the system PMMA/PDMS/THF at t = 30 °C, C_T = 1.33 × 10^{-2} g/cm^3, x = 0.90, and θ = 50°. The dots represent the experimental data and the solid line is a monoexponential fit. (b) Same as (a): double-exponential fit according to relation 10.

and the chosen one is that for P closest to 0.5.

$$\left(\frac{G^{(2)}(q,t)}{B} - 1\right)^{1/2} = \int_0^\infty A(\tau)e^{-(t/\tau)}\,d\tau = S_{11}(q,t) \qquad (9)$$

The analysis of the autocorrelation functions was made on-line with a Microvax II computer. The results obtained from this procedure of data treatment were quite similar to those obtained with a so-called Kohlrauch–Williams–Watts (KWW) function[61] extended to two relaxation processes, namely

$$S_{11}(q,t) = a_C \exp[-(t/\tau_{KWW,C})^{\beta_C}] + a_I \exp[-(t/\tau_{KWW,I})^{\beta_I}] \qquad (10)$$

where the β parameters ($0 < \beta_{C,I} \leq 1$) are directly related to the width of the distribution. The mean relaxation times $\bar{\tau}_{C,I}$ are given by

$$\bar{\tau}_C = \frac{\tau_{KWW,C}}{\beta_C}\Gamma(\beta_C^{-1}) \qquad (11)$$

$$\bar{\tau}_I = \frac{\tau_{KWW,I}}{\beta_I}\Gamma(\beta_I^{-1}) \qquad (12)$$

where $\Gamma(\beta_{C,I})$ denotes the Gamma function. It is important, however, to note that in this latter analysis the $\beta_{C,I}$ values were found to be very close to unity.

Results and Discussion

The experiments were performed at the temperature t = 30 ± 0.1 °C at several angles between 50 and 130° far from the phase separation and at one total polymer concentration, namely, C_T = 1.33 × 10^{-2} g/cm^3, which corresponds to $C_T/C^* \simeq 10$. A typical intensity autocorrelation function obtained from the ternary mixture PMMA/PDMS/THF at x = 0.90 and θ = 50° is displayed in Figure 4a. The dots represent the experimental data and the solid line a monoexponential fit. It is clear from the distribution of residuals, plotted at the top of Figure 4a, that the monoexponential fit is not satisfactory. Similar observations were made at the other compositions. Because of this unsatisfactory monoexponential fit, we analyzed the data with two exponential functions according to relation 10. Indeed, a good agreement was obtained between experimental data and the two-exponential fit as shown in Figure 4b. Values of β_C and β_I were found to be very close to unity. Additionally, Provencher's CONTIN[60] algorithm was used and the result of this analysis confirmed again that two relaxation processes characterize the dynamics of this system. The variations of the amplitudes (a_C, a_I) and the frequencies (Γ_C, Γ_I) of these two relaxation modes were considered as a function of composition x and scattering vector q.

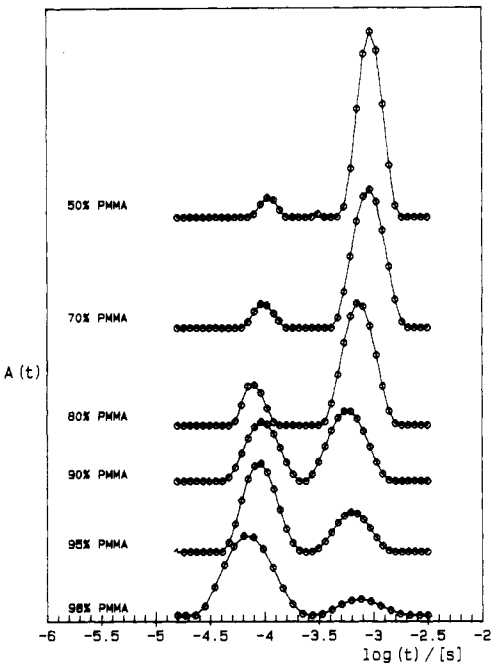

Figure 5. Relaxation time distribution obtained from CONTIN for the ternary mixtures PMMA/PDMS/THF at total polymer concentration C_T = 1.33 × 10^{-2} g/cm^3 and at the compositions $x = C_{PMMA}/C_T$ shown.

1. Amplitudes a_C and a_I: Effect of Composition. Figure 5 shows the variations of the two relaxation processes, represented by the two peaks, at θ = 50° as a function of composition ($0.5 \leq x < 1$) as detected by CONTIN analysis. It may be seen from this representation that the amplitude of the fast processes increases with the composition whereas at the same time one observes a decrease of the amplitude of the slow processes. At small composition, namely, $x < 0.1$, only the slow relaxation survives. This result at $x < 0.1$, already obtained for other systems,[18-34,36,37,41] is expected since the amplitude of the fast mode, a_C, tends to zero as the composition decreases, as shown in Figure 1. From this analysis we have plotted in Figure 6 the variation of the relative amplitude of the fast mode $a_C/(a_C + a_I)$ as a function of the composition $x = C_{PMMA}/C_T$. The dots represent the experimental data and the solid line represents the theoretical prediction.

Using eqs 2, 3, and 6, we obtain the best fit between experimental and theoretical results by adjusting the values of $\chi\Phi N$ and $V\Phi N$ in the expression

$$\frac{a_C}{a_C + a_I} = \frac{1}{1 + \left[\dfrac{(1-x)(1 + V\Phi N)}{x\{1 - 2x(1-x)\chi\Phi N\}}\right]} \qquad (13)$$

where we have taken $P(q) = 1$. This approximation is justified since at θ = 50°, $qR_g < 1$ and $P(q) \simeq 1$. Values

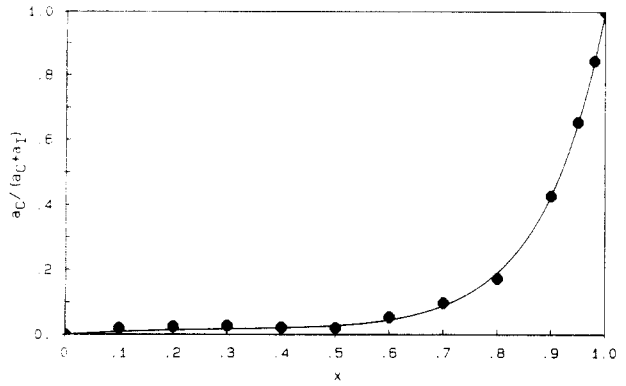

Figure 6. Variation of the relative amplitude of the fast mode $a_C/(a_C + a_I)$ as a function of the composition $x = C_{PMMA}/C_T$ at $C_T = 1.33 \times 10^{-2}$ g/cm^3 and $\theta = 50°$. The dots represent the experimental data and the solid line is the theoretical curve. The values of $\chi\Phi N \simeq 1.5$ and $V\Phi N \simeq 7.85$ correspond to the best fit according to eq 13.

of $(V\Phi N)_{exp} \simeq 7.85$ and $(\chi\Phi N)_{exp} \simeq 1.5$ have been obtained by using the nonlinear least-squares Marquardt algorithm with two independent adjustable parameters. Taking the theoretical expression $V\Phi N = 2A_2M_wC_T$, one obtains $(V\Phi N)_{theo} \simeq 5.24$. Within experimental error, this value is in the same order as that obtained by fitting the experimental data using relation 13. The values of $(V\Phi N)_{exp}$ and $(\chi\Phi N)_{exp}$ allow us to calculate the quantity $(\chi/V)_{exp} \simeq 0.19$. On the other hand, the relationship between χ/V and the second virial coefficients $A_{2,a}$, $A_{2,b}$, and $A_{2,ab}$ that characterize the thermodynamic interactions of the system is given by[48,50,51]

$$\frac{\chi}{V} = \frac{2m_am_bA_{2,ab}}{m_a^2A_{2,a} + m_b^2A_{2,b}} - 1 \qquad (14)$$

m_a and m_b are the molecular weights of the monomer units. From this relation, one obtains the value of $(A_{2,ab})_{exp} \simeq 3.38 \times 10^{-4}$ mol cm^3 g^{-2}, which is in good agreement with that obtained by static measurements.[55] Indeed, using the scaling law $\Delta A_2 = A_{2,ab} - (A_{2,a} + A_{2,b})/2 = (1.58 \pm 0.08) \times 10^{-2}M_w^{-0.4\pm0.05}$ [62] deduced from static measurements on the mixture PMMA/PDMS/chloroform in the so-called optical Θ conditions[63] where the determination of $A_{2,ab}$ is known with high precision, one obtains $A_{2,ab} \simeq 3.44 \times 10^{-4}$ mol cm^3 g^{-2}.

2. Frequencies: Angular Dependence. The angular variation of Γ_C and Γ_I has also been considered in the framework of this work. The experimental results are given in Figure 7. Whereas Γ_C is q^2 dependent for all of the compositions, Γ_I presents a strong deviation from the q^2 behavior as shown in parts a and b of Figure 7, respectively, for $x = 0.8$ as an example. This result has been also observed in PS/PMMA/toluene[50] and PS/PDMS/solvent[51] systems. Following the same procedure described in refs 50 and 51, the experimental data were fitted by using the relation

$$\Gamma_I(q) = q^2\frac{D_I}{P(q)} \qquad (15)$$

by adjusting the values of D_I and that of the apparent radius of gyration $R_{g,app}$ in the expression of the form factor $P(q)$ represented by the Debye function

$$P(q) = 2(e^{-u} + u - 1)/u^2 \qquad (16)$$

where $u = (qR_{g,app})^2$. The values of the apparent radius of gyration $R_{g,app}$ deduced from this analysis are listed in Table II and plotted as a function of the composition in Figure 8. This result shows that $R_{g,app}$ is strongly affected

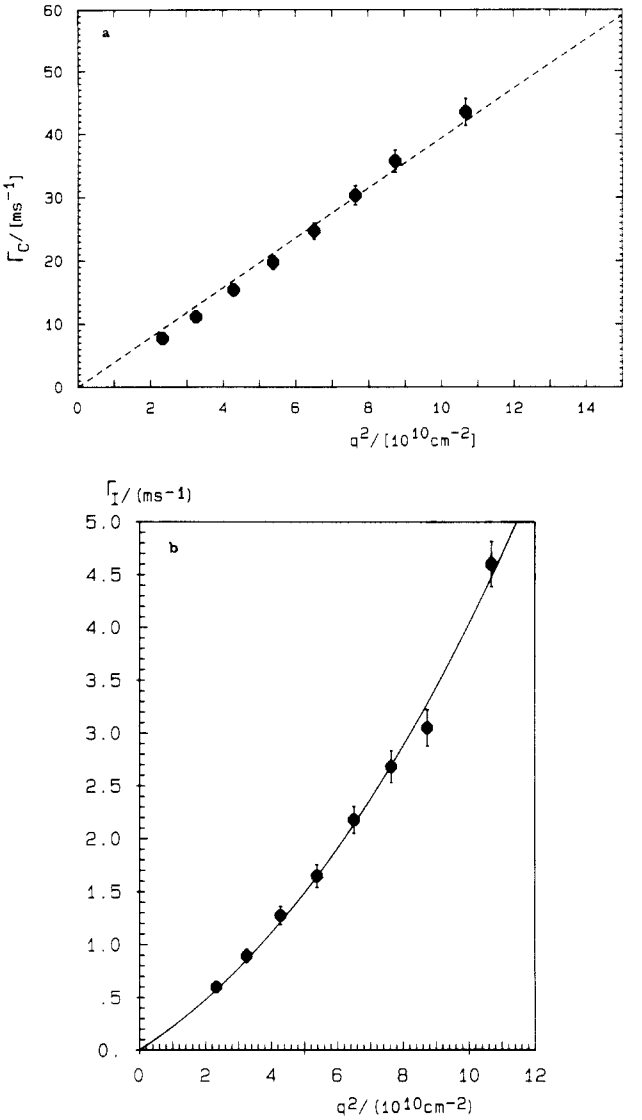

Figure 7. Variation of the relaxation frequencies Γ_C (a) and Γ_I (b) as a function of q^2 measured on the ternary system PMMA/PDMS/THF: $C_T = 1.33 \times 10^{-2}$ g/cm^3 and $x = 0.8$. The solid line (b) represents the best fit according to eqs 15–16.

Table II
Variation of $R_{g,app}$ as a Function of x

x	$R_{g,app}$, Å	x	$R_{g,app}$, Å
0.10	190.8	0.60	601.3
0.20	321.7	0.70	504.7
0.30	499.5	0.80	392.7
0.40	538.4	0.90	208.4
0.50	555.9		

by the properties of the system and particularly by the composition x as has been predicted[64] and reported for other systems.[65] Moreover, the value for the radius of gyration decreases with the concentration as has been reported for other systems.[66] Indeed, at infinite dilution $R_g = 583$ Å whereas at $C_T = 1.33 \times 10^{-2}$ g/cm^3 and $x = 0.5$, its value is 556 Å.

3. Diffusion Coefficients: Effect of Composition. Two relaxation processes characterized by their frequencies Γ_C and Γ_I were deduced from the analysis of the autocorrelation functions obtained from the PMMA/PDMS/THF system. The values of the associated diffusion coefficients $D_C = (\Gamma_C/q^2)_{q\to0}$ and $D_I = (\Gamma_I/q^2)_{q\to0}$ are plotted in Figure 9 as a function of the composition of the "visible" polymer x.

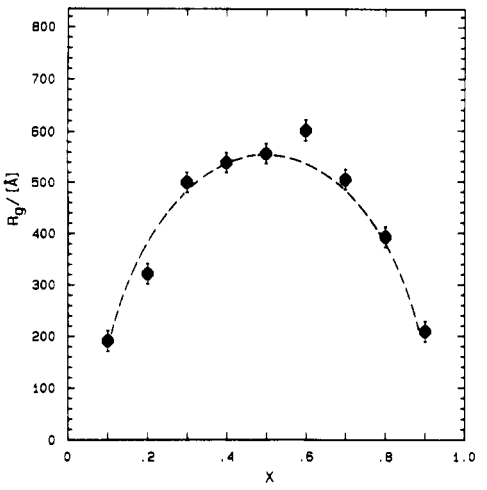

Figure 8. Experimental variation of the apparent radius of gyration deduced from the best fit of Γ_I as a function of q^2 according to eq 15 and 16. The dashed line is a guide for the eyes.

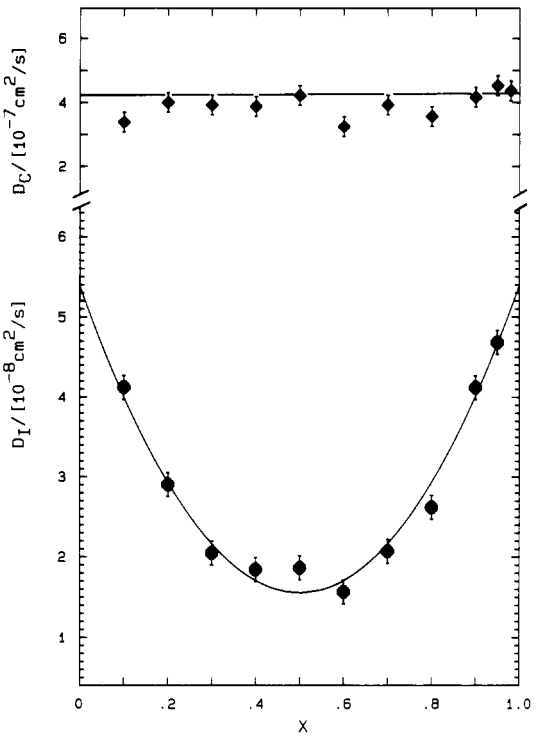

Figure 9. Variation of the diffusion coefficients D_C (top) and D_I (bottom) as a function of the composition $x = C_{PMMA}/C_T$ at $C_T = 1.33 \times 10^{-2}$ g/cm^3. The dots represent the experimental data and the solid line is the theoretical variation of D_I. The values of $\chi\Phi N \simeq 1.43$ and $D_S \simeq 5.39 \times 10^{-8}$ cm s^{-1} correspond to the best fit according to eq 17.

(i) Cooperative Diffusion Coefficient D_C. At the top of Figure 9 are plotted the experimental values of D_C as a function of x. Within experimental error, D_C is found to be insensitive to the composition of the "visible" polymer in the mixture. Moreover, the value of D_C obtained from the ternary mixture is identical with that measured in the corresponding binary system PMMA/THF (e.g., $x = 1$), namely, $D_C \simeq 4.22 \times 10^{-7}$ cm^2/s. This result, which is also reported for other systems,[44-51] confirms again the theoretical prediction and the physical nature attributed to this fast-relaxation process called the cooperative diffusion mode.

(ii) Interdiffusion Coefficient D_I. The variation of D_I with x is plotted at the bottom of Figure 9. The dots represent the experimental data and the solid line represents the theoretical variation. The best fit between experiment and theory using eqs 5–7 is obtained by adjusting the values of $\chi\Phi N$ and the self-diffusion coefficient D_S in the expression

$$D_I = D_S[1 - 2x(1-x)\chi\Phi N] \quad (17)$$

Values of $(\chi\Phi N)_{exp} \simeq 1.43$ and $D_S \simeq 5.39 \times 10^{-8}$ cm^2 s^{-1} have been obtained by using the nonlinear least-squares Marquardt algorithm with two independent adjustable parameters. The value of $\chi\Phi N$ is nearly identical with that obtained by fitting the experimental data for $a_C/(a_C + a_I)$, namely, $\chi\Phi N \simeq 1.5$ (see relation 13 and Figure 6). One notes that the determination of the self-diffusion coefficient was always an extrapolation to an infinitely dilute system ($C_T \to 0$). In this experiment we have shown that also an extrapolation to zero composition at constant total polymer concentration C_T is a direct determination of the self-diffusion coefficient (see relations 5–7 and Figure 2b). Experiments using pulsed-field-gradient NMR and forced Rayleigh scattering (FRS) will provide some information on the dynamics of the system and allow comparison of the self-diffusion coefficients obtained from these techniques.

Conclusion

In this work we have investigated the dynamics of ternary mixtures of PMMA/PDMS/THF using quasi-elastic light scattering. THF is a good solvent for both polymers and is isorefractive with PDMS. At one total polymer concentration, in the semidilute range and far from the "cloud point" ($C^* \leq C_T < C_{sp}$), the effects of composition of the "visible" polymer $x = C_{PMMA}/C_T$ and the wave vector q were considered. After careful data treatment of the autocorrelation functions as measured by QELS using CONTIN, it comes out clearly that two processes characterize the dynamics of this system. The first mode, Γ_C, which is fast, is not sensitive to the composition and the associated diffusion coefficient $D_C = (\Gamma_C/q^2)_{q\to 0}$ is equal to the only relaxation process, D_C, measured in the corresponding binary system PMMA/THF. This result confirms the theoretical interpretation given to this mode as a cooperative diffusion process reflecting the motion of the pseudonetwork formed by all the chains present within the system. The second mode, which is slow and called the interdiffusion mode, is sensitive to the composition and reflects the motion of one species with respect to the other. The extrapolation of D_I to zero composition gives us the value of the self-diffusion coefficient D_S of "one" PMMA chain in a matrix of PDMS. This diffusion coefficient is known as being the tracer diffusion coefficient D_{tr}. Its value may be also measured by pulsed-field-gradient NMR and FRS.

Regarding the variation of the amplitudes of these two processes, the results show a good agreement with the theoretical predictions. Indeed, for small values of composition ($x < 0.1$) only the slow mode survives, while for large x, the fast mode dominates. In the intermediate range, both processes emerge together until reaching the same order of magnitude ($a_C = a_I$), which corresponds to the ideal conditions to observe the two relaxation modes simultaneously. From this analysis, the value of the second virial coefficient $A_{2,ab}$ is deduced, and the result is in good agreement with that obtained by a direct static light scattering measurement in the so-called optical Θ condition.

The variation of Γ_C with q^2 is linear while the behavior of Γ_I with q^2 is significantly nonlinear. This deviation is directly related to the static properties of the system. Indeed, the apparent radius of gyration deduced from this

analysis is sensitive to the composition x according to the theoretical predictions.[64,65]

In conclusion, most of the experimental data obtained from the ternary mixtures PMMA/PDMS/THF are consistent with the simple mean field developed by Benoit and Benmouna and confirm again the use of the dynamic RPA equations. This conclusion was also drawn for other systems (e.g., PS/PMMA/toluene,[49,50,52] PS/PDMS/solvent,[51] and PIB_1/PIB_2/chloroform[53,54]).

Finally, it may be mentioned that with regard to the theory of dynamics in ternary systems, there exists a different approach by Akcasu and Tombakoglu.[67] We did not take into account this recent theory since our experimental results were found to be in good agreement with the theoretical results of Benmouna, Benoit, and co-workers.[44-49]

Acknowledgment. We express our gratitude to Professors H. Benoit and M. Benmouna, M. Duval for fruitful discussions, and M. G. Brereton, T. A. Vilgis, and M. Schmidt for their interest and valuable comments on this work. We also thank very much Professor A. Z. Akcasu for sending a preprint of ref 67. R.B. acknowledges the support of the Max-Planck-Gesellschaft. We thank B. Momper and T. Wagner for preparing the PDMS sample.

References and Notes

(1) Jannink, G.; de Gennes, P.-G. *J. Chem. Phys.* **1968**, *48*, 2260.
(2) Brochard, F.; de Gennes, P.-G. *Physica* **1983**, *118A*, 289.
(3) Binder, K. *J. Chem. Phys.* **1983**, *79*, 6387.
(4) Brochard, F.; Jouffroy, J.; Lovinson, P. *Macromolecules* **1983**, *16*, 1638.
(5) Brochard, F.; Jouffroy, J.; Lovinson, P. *Macromolecules* **1984**, *17*, 2925.
(6) Kramer, E.; Green, P.; Palmstrøm, C. *Polymer* **1984**, *25*, 473.
(7) Sillescu, H. *Macromol. Chem.* **1984**, *5*, 519.
(8) Green, P. F.; Palmstrøm, Ch. J.; Mayer, J. W.; Kramer, E. *Macromolecules* **1985**, *18*, 501.
(9) Akcasu, A. Z.; Benmouna, M.; Benoit, H. *Polymer* **1986**, *27*, 1935.
(10) Brereton, M. G.; Fischer, E. W.; Fytas, G.; Murschall, U. *J. Chem. Phys.* **1987**, *86*, 5174.
(11) Composto, R. J.; Kramer, E. J.; White, D. M. *Nature* **1987**, *328*, 234.
(12) Phillies, G. D. J. *J. Chem. Phys.* **1974**, *60*, 983.
(13) Phillies, G. D. J. *Biopolymers* **1975**, *14*, 499.
(14) Pusey, P. N.; Fijnaut, H. M.; Vrij, A. *J. Chem. Phys.* **1982**, *77*, 4270.
(15) Phillies, G. D. J. *J. Chem. Phys.* **1983**, *79*, 2325.
(16) Akcasu, A. Z.; Hammouda, B.; Lodge, T. P.; Han, C. C. *Macromolecules* **1984**, *17*, 759.
(17) Foley, G.; Cohen, C. *Macromolecules* **1987**, *20*, 1891.
(18) Cotts, D. B. *J. Polym. Sci., Polym. Phys. Ed.* **1983**, *21*, 1381.
(19) Hanley, B.; Balloge, S.; Tirrell, M. *Chem. Eng. Commun.* **1983**, *24*, 93.
(20) Lodge, T. P. *Macromolecules* **1983**, *16*, 1393.
(21) Martin, J. E. *Macromolecules* **1984**, *17*, 1279.
(22) Hanley, B.; Tirrell, M.; Lodge, T. P. *Polym. Bull. (Berlin)* **1985**, *14*, 137.
(23) Lodge, T. P. *Macromolecules* **1986**, *19*, 2986.
(24) Martin, J. E. *Macromolecules* **1986**, *19*, 922.
(25) Martin, J. E. *Macromolecules* **1986**, *19*, 1281.
(26) Lodge, T. P.; Wheeler, L. M. *Macromolecules* **1986**, *19*, 2983.
(27) Wheeler, L. M.; Lodge, T. P.; Hanley, B.; Tirrell, M. *Macromolecules* **1987**, *20*, 1120.
(28) Chang, T.; Han, C. C.; Wheeler, L. M.; Lodge, T. P. *Macromolecules* **1988**, *21*, 1870.
(29) Hadgraft, J.; Hyde, A. J.; Richard, R. W. *J. Chem. Soc., Faraday Trans. 2* **1979**, *75*, 1495.
(30) Kuwamoto, K.; Numasawa, N.; Nose, T. *Rep. Prog. Polym. Phys. Jpn.* **1984**, *27*, 507.
(31) Nemoto, N.; Inoue, T.; Makita, Y.; Tsunashima, Y.; Kurata, M. *Macromolecules* **1985**, *18*, 2516.
(32) Nemoto, N.; Okada, S.; Inoue, T.; Tshunashima, Y.; Kurata, M. *Macromolecules* **1986**, *19*, 2305.
(33) Numasawa, N.; Kuwamoto, K.; Nose, T. *Macromolecules* **1986**, *19*, 2593.
(34) Chu, B.; Wu, D.-Q.; Liang, G.-M. *Macromolecules* **1986**, *19*, 2665.
(35) Chu, B.; Wu, D.-Q. *Macromolecules* **1987**, *20*, 1606.
(36) Nemoto, N.; Okada, S.; Inoue, T.; Kurata, M. *Macromolecules* **1988**, *21*, 1502.
(37) Nemoto, N.; Okada, S.; Inoue, T.; Kurata, M. *Macromolecules* **1988**, *21*, 1509.
(38) Brown, W.; Rymden, R. *Macromolecules* **1988**, *21*, 840.
(39) Nemoto, N.; Inoue, T.; Makita, Y.; Tsunashima, Y.; Kurata, M. *Macromolecules* **1984**, *17*, 2629.
(40) Von Meerwall, E. D.; Amis, E. J.; Ferry, J. D. *Macromolecules* **1985**, *18*, 260.
(41) Kim, H.; Chang, T.; Yohanan, J. M.; Wang, L.; Yu, H. *Macromolecules* **1986**, *19*, 2737.
(42) de Gennes, P.-G. *Scaling Concepts in Polymer Physics*; Cornell University Press: Ithaca, NY, 1979.
(43) Hess, W. *Macromolecules* **1986**, *19*, 1395.
(44) Benmouna, M.; Benoit, H.; Duval, M.; Akcasu, A. Z. *Macromolecules* **1987**, *20*, 1107.
(45) Benmouna, M.; Benoit, H.; Borsali, R.; Duval, M. *Macromolecules* **1987**, *20*, 2620.
(46) Benmouna, M.; Duval, M.; Borsali, R. *J. Polym. Sci., Polym. Phys. Ed.* **1987**, *25*, 1839.
(47) Benmouna, M.; Duval, M.; Borsali, R. *Macromolecules* **1988**, *21*, 520.
(48) Borsali, R. Ph.D. Thesis, University of Strasbourg, Strasbourg, France, 1988.
(49) (a) Borsali, R.; Duval, M.; Benoit, H.; Benmouna, M. *Macromolecules* **1987**, *20*, 1112. (b) Borsali, R.; Vilgis, T. A. *J. Chem. Phys.*, in press.
(50) Borsali, R.; Duval, M.; Benmouna, M. *Polymer* **1989**, *30*, 610.
(51) Borsali, R.; Duval, M.; Benmouna, M. *Macromolecules* **1989**, *22*, 816.
(52) Konack, C.; Tuzar, Z.; Jakes, J., preprint (submitted to *Polymer*).
(53) (a) Brown, W.; Zhou, P. *Macromolecules* **1989**, *22*, 3508. (b) Brown, W.; Zhou, P. *Macromolecules* **1989**, *22*, 4031.
(54) Brown, W.; Konack, C.; Johnsen, M.; Zhou, P., preprint (submitted to *Macromolecules*).
(55) Anasagasti, M.; Katime, I.; Strazielle, C. *Makromol. Chem.* **1987**, *188*, 201.
(56) Yamakawa, H. *Modern Theory of Polymer Solutions*; Harper and Row: New York, 1982.
(57) Lapp, A.; Herz, J.; Strazielle, C. *Makromol. Chem.* **1985**, *186*, 1919.
(58) $C^* = 3M_w/[N_A(4\pi R_g^3)]$.
(59) Siegert, A. J. F. *MIT Rad. Lab. Rep.* **1943**, *No. 465*.
(60) (a) Provencher, S. W.; Hendrix, J.; De Maeyer, L.; Paulussen, N. *J. Chem. Phys.* **1978**, *69*, 4273. (b) Provencher, S. W. *Makromol. Chem.* **1979**, *180*, 201. (c) Provencher, S. W. *Comput. Phys. Commun.* **1982**, *27*, 213. (d) Provencher, S. W. *Comput. Phys. Commun.* **1982**, *27*, 229.
(61) See, for example: Patterson, G. D. *Adv. Polym. Sci.* **1983**, *48*, 175.
(62) Ould-Kaddour, L. Thesis, University of Strasbourg, Strasbourg, France, 1988.
(63) Fukuda, T.; Nagata, M.; Inagaki, H. *Macromolecules* **1984**, *17*, 548.
(64) Benoit, H.; Benmouna, M. *Macromolecules* **1984**, *17*, 535.
(65) Ould-Kaddour, L.; Strazielle, C. *Polymer* **1987**, *28*, 459.
(66) Daoud, M.; Cotton, J. P.; Farnoux, B.; Jannink, G.; Sarma, G.; Benoit, H.; Duplessix, R.; Picot, C.; de Gennes, P.-G. *Macromolecules* **1975**, *8*, 804.
(67) Akcasu, A. Z.; Tombakoglu, M. *Macromolecules* **1990**, *23*, 607.